RSC Advances




ROYAL SOCIETY OF CHEMISTRY

www.rsc.org/advances

Cite this: DOI: 10.1039/c0xx00000x

www.rsc.org/xxxxxx

ARTICLE TYPE

# Dinuclear Cd(II), Mn(II) and Cu(II) complexes derived from (anthraquinone-1-diyl) benzoate: DNA binding and cleavage studies

**Lin Liu,[a,†] Gong-Ming Zhang,[a,†] Ru-Gang Zhu,[*b] Yong-Hui Liu,[b] Hui-Meng Yao,[a] Zheng-Bo Han[*a]**

***Received (in XXX, XXX) Xth XXXXXXXXX 20XX, Accepted Xth XXXXXXXXX 20XX***

**DOI: 10.1039/b000000x**

Three dinuclear complexes with the formulas $[Cd_2(L_1)_4(DMF)_2(H_2O)_2]\cdot$(**1**), $[Mn_2(L_1)_4(DMF)_2(H_2O)_2]\cdot$(**2**), $[Cu_2(L_2)_4(EtOH)(H_2O)]\cdot 2DMF$ (**3**) ($L_1$ = 3-(anthraquinone-1-diyl) benzoate, $L_2$ = 4-(anthraquinone-1-diyl)benzoate), have been successfully synthesized under solvothermal conditions. The characterizations of thermogravimetric analysis, PXRD patterns and IR spectra of **1**-**3** were carried out. The oxidation state of the Mn(II) and Cu(II) atoms was confirmed by the magnetic studies. The Cu(II) complex has the activity for DNA cleavage. The supercoiled DNA was completely degraded to nicked DNA (72%) and linear DNA (38%) with 1 μg/μL Cu(II) complex for 2 h at pH 7.0. The DNA cleavage by Cu(II) complex was likely to proceed via a hydrolytic degradation pathway.

## Introduction

The dinuclear metal complexes are well-known as artificial metallonucleases and metalloproteases.[1,2] Over the past decade, the transition metal based dinuclear complexes have seen sustained progress in the complexation and supermolecule chemistry.[3] This is mainly due to the rapid development of biomedical applications of transition metal systems. Transition metal complexes can act as highly useful probes for biological macromolecules, and some of them show high activities with DNA.[4–8] Metal complexes have the capacity to cause DNA damage by photoinduced oxidative strand breakage due to their photophysical and redox activities,[9,10] and to mediate charge transport through DNA.[11,12] Intercalative binding by metal complexes can disrupt the helical nature of DNA; make crucial impact on DNA integrity and cell viability.[13] The researches of DNA interactions with transition metal complexes continue to be a vibrant area for their potential applications on anticancer pharmaceuticals, diagnostics, signaling, and therapeutic applications.[14,15] Cu(II) complexes containing phenanthroline showed excellent DNA cleavage activity and had been used as artificial nucleases in nucleic acid chemistry.[16–28] The DNA cleavage reactions are found to proceed via different mechanism pathways on UV or red-light irradiation.[29]

In this work, we report the synthesis and structural characterization of three dinuclear Cd(II), Mn(II) and Cu(II) complexes, namely, $[Cd_2(L_1)_4(DMF)_2(H_2O)_2]$ (**1**), $[Mn_2(L_1)_4(DMF)_2(H_2O)_2]$ (**2**), $[Cu_2(L_2)_4(EtOH)(H_2O)]\cdot 2DMF$ (**3**) ($L_1$ = 3-(anthraquinone-1-diyl) benzoate, $L_2$ = 4-(anthraquinone-1-diyl) benzoate, the structure is illustrusted in **Scheme 1**). The DNA cleavages of complexes **1-3** were studied, the results showed that only the Cu(II) complex has the activity for DNA cleavage.

## Experimental Section

### Materials and Methods

Glycol dimethyl ether (DME) were further purified, other chemicals purchased of reagent grade and were used without further purification. The supercoiled pBR 322 DNA used for DNA cleavage reactions were purchased from Takara (China). Elemental analyses (C, H, N) were performed on a Perkin-Elmer 2400 CHN elemental analyzer. FT/IR spectra were recorded in the range 4000-400 $cm^{-1}$ on an Alpha Centaut FT/IR spectrophotometer using a KBr pellet. Thermogravimetric analyses (TGA) were taken on a Perkin-Elmer Pyrisl (25-900 $^oC$, 5 $^oC$ $min^{-1}$, flowing $N_2$ (g)). X-ray powder diffraction was recorded with a Bruker AXS D8 advanced automated diffractometer with Cu-K$\alpha$ radiation. The magnetic data were collected on a Quantum Design MPMS SQUID-XL-5 magnetometer using the crushed single-crystal samples. Magnetic data were corrected for the diamagnetic contribution calculated from Pascal constants[30] and a background of the sample holder. Fluorescence spectra were measured on an F-7000 FL spectrophotometer in the solid state at room temperature.

### Synthesis of $HL_1$ and $HL_2$

$HL_1$: 1-bromoanthraquinone (1.02 g, 0.0039 mol), 3-methoxycarbonylphenylboronic acid (3.5 g, 0.019 mol), CsF (5.77 g) and $Pd(PPh_3)_4$ (0.4 g) were mixed in a two-necked schlenk flask and vacuumed for 30 minutes. 200 mL degassed $CH_3OCH_2CH_2OCH_3$ (DME) was added through a canula. The mixture was heated to reflux under $N_2$ (g) for 48 hours. The distilled water was added after the mixture was cooled to room temperature. The water phase was extracted with $CH_2Cl_2$. The mixed organic phases were dried with $MgSO_4$. After the solvent was removed, the crude product was purified by column chromatography (silica, Ethyl acetate: petroleum ether (v/v) = 1:4) to give the pure product. The product of esters was dissolved in 100 mL mixture of THF and MeOH (v/v = 1:1), 20 mL 2 N NaOH aqueous solution was added. The mixture was stirred at 343 K overnight. The organic phase was removed. The aqueous phase was acidified with diluted hydrochloric acid to give yellow

precipitate, which was filtered and washed with distilled water several times. $^1$HNMR (300 MHz, DMSO): 3-(anthraquinone-1-diyl) methyl benzolic acid, 7.56 (m, 2 H), 7.67 (dd, 1 H), 7.89 (m, 4 H), 7.97(m, 2 H), 8.18 (m, 1 H), 8.30 (dd, 1 H) (Fig. S1).

$HL_2$: Synthesis of and $HL_2$ was similar to that of $HL_1$ except that 4-methoxycarbonylphenylboronic acid (3.5 g, 0.019 mol) was used instead of 3-methoxycarbonylphenylboronic acid. NMR (300 MHz, DMSO): 4-(anthraquinone-1-diyl) methyl benzoic acid, 7.45 (d, 2 H), 7.67 (dd, 1 H), 7.90 (m, 3 H), 7.99(m, 3 H), 8.20 (m, 1 H), 8.33 (dd, 1 H) (Fig. S2).

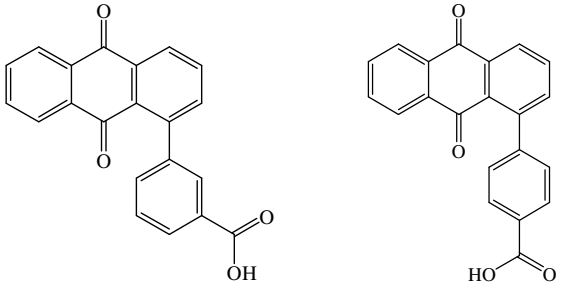


$HL_1$ $HL_2$

**Scheme 1**

**Table 1** Crystal data and structure refinement for **1**, **2** and **3**

| | **1** | **2** | **3** |
|---|---|---|---|
| Empirical formula | $C_{45}H_{31}CdNO_{10}$ | $C_{45}H_{31}MnNO_{10}$ | $C_{46}H_{33}CuNO_{10}$ |
| Formula weight | 858.11 | 800.65 | 823.27 |
| Crystal system | Triclinic | Triclinic | Triclinic |
| Space group | *P*-1 | *P*-1 | *P*-1 |
| *a*/ Å | 8.0107(19) | 8.012(6) | 11.554(9) |
| *b*/ Å | 14.519(4) | 14.559(14) | 12.053(9) |
| *c*/ Å | 17.487(4) | 17.184(14) | 15.546(11) |
| $\alpha$/ deg | 109.295(3) | 108.545(12) | 75.142(9) |
| $\beta$/ deg | 97.629(3) | 97.460(9) | 71.824(8) |
| $\gamma$/ deg | 103.764(3) | 103.804(9) | 86.856(9) |
| *V*/Å$^3$ | 1814.3(8) | 1799(3) | 1987 (3) |
| *Z* | 2 | 2 | 2 |
| *Dc*/mg cm$^{-3}$ | 1.571 | 1.478 | 1.376 |
| $\mu$/ mm$^{-1}$ | 0.668 | 0.427 | 0.611 |
| Range for data collection/$^o$ | 1.56-26.00 | 2.3-25.8 | 1.856-25.995 |
| Collected reflections | 11269 | 11107 | 12135 |
| Data / restraints / parameters | 6994 / 14 / 515 | 6916 / 13 / 510 | 7596 / 0 / 533 |
| *F*(000) | 872 | 826 | 850 |
| Final *R* indices [$I > 2\sigma(I)$][a] | $R_1 = 0.0463$, w$R_2 = 0.1180$ | $R_1 = 0.0604$, w$R_2 = 0.1582$ | $R_1 = 0.0444$, w$R_2 = 0.1292$ |
| Goodness-of-fit on $F^2$ | 1.026 | 1.020 | 1.022 |
| R indices (all data) | $R_1 = 0.0597$, w$R_2 = 0.1272$ | $R_1 = 0.0832$, w$R_2 = 0.1758$ | $R_1 = 0.0544$, w$R_2 = 0.1377$ |
| largest diff. peak and hole(e Å$^{-3}$) | 0.963, -0.482 | 0.918, -0.599 | 0.703, -0.356 |

[a] $R_1 = \sum||F_o|-|F_C||/\sum|F_o|$; $wR_2 = \sum[w(F_o^2-F_c^2)^2]/\sum[w(F_o^2)^2]^{1/2}$

**Solvothermal Synthesis of complexes 1, 2 and 3**

$[Cd_2(L_1)_4(DMF)_2(H_2O)_2]$ (**1**): A mixture of $Cd(NO_3)_2{\cdot}4H_2O$ (0.00486 mmol, 0.015 g), $HL_1$ (0.0015 mmol, 0.005 g), DMF (1 mL) and $H_2O$ (0.5 mL) was stirred for 5 minutes in glass vial at room temperature, which was heated in an oven to 348 K for 3

days, followed by slowly cooling (5 K $h^{-1}$). The resulting yellow crystals were washed with DMF and dried in air (yield: *ca.* 67 %). Anal. cald(%) for **1** $C_{90}H_{62}Cd_2N_2O_{20}$: C, 62.98; H, 3.64; N, 1.63%. Found: C, 62.69; H, 3.74; N, 1.82.%. IR (KBr Pellets, $cm^{-1}$) : 3427 (m), 1673 (s), 1540 (s), 1568 (w), 1275 (s), 1384 (vs), 690 (s).

$[Mn_2(L_1)_4(DMF)_2(H_2O)_2]$ (**2**): Synthesis of **2** was similar to that of **1** except that $Mn(CH_3COO)_2{\cdot}4H_2O$ (0.006 mmol, 0.015 g) was used instead of $Cd(NO_3)_2{\cdot}4H_2O$. The resulting yellow crystals were washed with DMF and dried in air (yield: *ca.* 56 %). Anal. cald(%) for **2** $C_{90}H_{62}Mn_2N_2O_{20}$: C, 67.50; H, 3.90; N,1.75%. Found: C, 67.46; H, 4.12; N,1.86.%. IR (KBr Pellets, $cm^{-1}$): 3427 (m), 1672 (s), 1542 (w), 1275 (w), 1384 (vs), 710 (w).

$[Cu_2(L_2)_4(EtOH)(H_2O)]{\cdot}2DMF$ (**3**): $Cu(NO_3)_2{\cdot}3H_2O$ (0.006 mmol, 0.015 g) and $HL_2$ (0.0015 mmol, 0.005 g) were mixed and dispersed in DMF/EtOH(1.5 mL, 2:1 v/v), was stirred for 5 minutes in a glass vial at room temperature. Then, the solution was heated in an oven to 348 K for 3 days followed by slowly cooling (5 K $h^{-1}$). The resulting green crystals were washed with DMF and dried in air (yield: *ca.* 58 %). Anal. Cald (%) for **3** $C_{92}H_{66}Cu_2N_2O_{20}$: C, 67.11; H, 4.04; N, 1.70%. Found: C, 66.91; H, 3.93; N, 1.86%. IR (KBr Pellets, $cm^{-1}$) : 3438 (m), 1673 (s), 1655 (w), 1618 (w), 1276 (s), 1406 (s), 709 (s).

**X-ray Crystallography**

Crystallographic data of **1**, **2** and **3** were collected at room temperature with a Bruker Apex II CCD diffractometer with Mo-K$\alpha$ radiation ($\lambda$ = 0.71073 Å) and graphite monochromator using the $\omega$-scan mode. The structure was solved by direct methods and refined on $F^2$ by full-matrix least squares using SHELXTL.[31] Further details of the X-ray structural analyses are summarized in Table 1. The selected bond lengths and bond angles are shown in Table S1. The CCDC reference numbers are 1016792-1016794 for **1-3**. Copy of the data can be obtained free of charge on application to CCDC, 12 Union Road, Cambridge CB2 1EZ, UK [Fax: int code +44(1223)336-033; E-mail: deposit@ccdc.cam.ac.uk]

**DNA binding studies by competitive fluorescence displacement assay**

DNA and ethidium bromide (EB) were combined to give 10 mL of reaction mixture containing 1.1 μmol/L ethidium bromide, 3.9 μmol/L CT DNA and various concentrations of the complexes (from 0 to 30 μmol/L). Noncovalent interactions of complexes with double-stranded DNA were studied by measuring the decrease in fluorescence intensities.

**DNA Cleavage**

The reaction mixture (50 μL of total volume) containing 0.5 μg plasmid DNA pBR322 and 20 mM HEPES buffer (pH 7.0), were incubated in an eppendorf tube at 37°C for a defined time, and then quenched by the addition of 5 μL of loading buffer (0.25% bromophenol blue, 0.25% xylene cyanol, 30% glycerol, and 10 mM EDTA).

The 25 μL sample was loaded directly onto a 0.9% agarose gel containing ethidium bromide (1 μg/mL) and then electrophoresed at a constant voltage of 70 mV for 120 min in TBE buffer (90 mM Tris-borate, pH 8.0, 20 mM EDTA). The gels were photographed under UV light and quantitation of cleavage products was performed by Glyko BandScan software, Version 4.30. Supercoiled plasmid DNA values were corrected by a factor 1.3, based on average literature estimate of lowered binding of ethidium to this structure.[32]

## Results and Discussion

**Crystal structures**

The solvothermal reaction of $HL_1$ or $HL_2$ with $Cd(NO_3)_2{\cdot}4H_2O$, $Mn(CH_3COO)_2{\cdot}4H_2O$, $Cu(NO_3)_2{\cdot}3H_2O$ with the presence of DMF and EtOH lead to the generation of complexes **1**-**3**.

$[Cd_2(L_1)_4(DMF)_2(H_2O)_2]$ (**1**) and $[Mn_2(L_1)_4(DMF)_2(H_2O)_2]$ (**2**): Single-crystal X-ray analysis reveals that complexes **1** and **2** are isomorphous, so only the structure of **1** is described here. **1** is a dinuclear Cd(II) complex, which crystallizes in triclinic space group *P*-1 (Table 1). There are one crystallographically independent Cd(II) center, two $L_1$ ligands, one aqua ligand and one coordinated DMF molecule in the asymmetric unit. The Cd1 center is hepta-coordinate and surrounded by five carboxylate oxygen atoms, one aqua ligands and one DMF molecule to form pentagonal bipyramid geometry. In **1**, $L_1$ ligand adopts two kinds of coordination modes: chelating and $\mu_2$-O; $\kappa^2$O, O' coordination modes. Two Cd(II) centers are connected by four carboxylate groups of $L_1$ ligands via two chelating and two $\mu_2$-O; $\kappa^2$O, O' coordination modes to form a dinuclear Cd(II) complex (Fig. 1a). Intermolecular hydrogen bonds between the coordinated water molecules and the carboxylate oxygen atoms (O1 and O5) define an interaction with an O···O distance of 2.846(5) and 2.854(5) Å. The hydrogen bonds link the adjacent dinuclear Cd(II) moieties to form a 1D ribbon structure (Fig. 1b; Table S2). Furthermore, adjacent 1D ribbons are connected together via π-π stacking interaction, forming a 3D supermolecule framework (Fig. 1c).

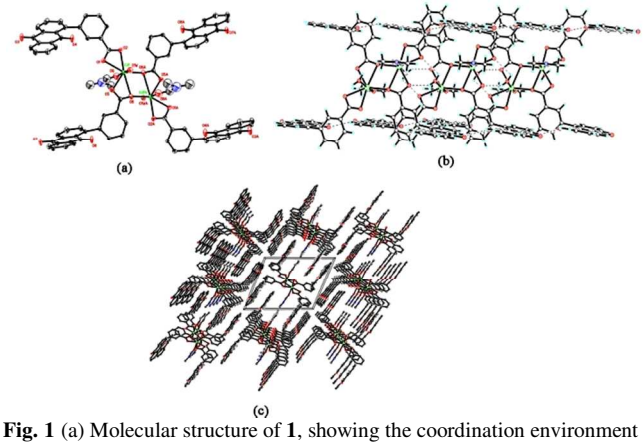


**Fig. 1** (a) Molecular structure of **1**, showing the coordination environment of Cd(II) and the coordination mode of the $L_1$ ligands. All hydrogen atoms are omitted for clarity. (b) Hydrogen-bonded 1D ribbon chain fragment showing the labelling C-H···O and O-H···O hydrogen bonds. (c) 3D stacking plot assembled by 1D ribbons and π–π stacking interactions. Symmetry transformations used to generate equivalent atoms: A 1-x, -y, 1-z.

$[Cu_2(L_2)_4(EtOH)(H_2O)]{\cdot}2DMF$ (**3**): Single-crystal X-ray diffraction analysis indicates that **3** features a dinuclear Cu(II) paddle wheel structure with the formula $C_{90}H_{62}Mn_2N_2O_{20}$ (Fig. 2a). There is one crystallographically independent Cu(II) center, two $L_2$ ligand, half water molecule and half EtOH with the occupancy of 0.5, and one free DMF molecule in the asymmetric unit. Two Cu(II) centers are connected by four carboxylate groups of $L_2$ ligands via bidentate coordination mode to form a dinuclear paddle wheel Cu(II) complex. π-π stacking interactions

from adjacent dinuclear units can be observed in rings from lateral $L_2$ ligands with a perpendicular separation of 3.421-3.503 Å, a centroid-to-centroid distance of 3.7142-3.8195 Å and slip angle (the angle between the centroid vector normal to the plane) of 9.07-23.45°. These values are typical aromatic π-π stacking interactions (Table S3). Atom C4 of $L_1$ ligand also have weak interactions with $L_2$ aromatic ring, the data is listed in Table S4. Adjacent dinuclear Cu2 units are further linked by π-π stacking interactions and weak interactions to form a 1D ribbon (Fig. 2b). Furthermore, 1D ribbons are linked by hydrogen bonds to construct a 3D supermolecule network (Table S5). These weak interactions enhance the stability of the complex.

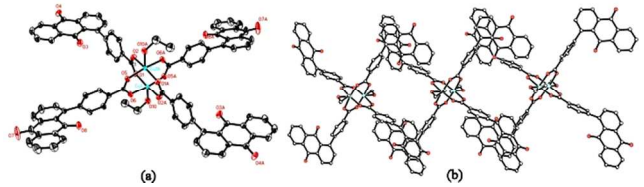


**Fig. 2** (a) Ellipsoids drawing of the coordination environments of Cu(II) and the bridging mode of the $L_2$ ligand in **3**. All hydrogen atoms are omitted for clarity.(b)1D ribbon chain constructed by π–π stacking interaction.

**Thermogravimetric analysis, PXRD patterns and IR spectra of 1-3**:

The thermal stability of **1** and **3** was examined by TGA in a dry nitrogen atmosphere from 35 to 900 °C (Fig. S3). The results indicate that the coordinated DMF molecules and the aqua ligands lose in the temperature range of 20 to 300°C (calcd/found: 10.60/10.31%), and then began to decompose upon further heating. The TG pattern of Complex **3** is shown in Fig. S3b. The first step from 25-254 °C with ca. 12.77 % loss could be attributed to the loss of the guest DMF molecules, coordinated EtOH and $H_2O$ molecules (the weight ca. 11.09 %), the frameworks of complexes **3** begin to decompose upon further heating. The PXRD patterns of **1-3** (Fig. S4) show that the diffraction patterns are almost the same as the simulated ones, indicating the phase purity of the products. The differences in intensity may be due to the preferred orientation of the powder samples.[33,34]

The IR spectrum of **1** shows characteristic bands of carboxyl groups at 1673 $cm^{-1}$ ($\nu_{as}$) and 1540 $cm^{-1}$($\nu_s$) The separations (Δ) of $\nu_{as}$ ($CO_2$) indicate the presence of chelating (133 $cm^{-1}$) coordination mode in **1**. The IR spectrum of **2** indicates characteristic bands of carboxyl groups at 1673 $cm^{-1}$($\nu_{as}$) , 1541 $cm^{-1}$ ($\nu_s$) and 1384 $cm^{-1}$ ($\nu_s$). The separations (Δ) between $\nu_{as}$ ($CO_2$) and $\nu_s$ ($CO_2$) indicate the presence of chelating (132 $cm^{-1}$) and bidentate (289 $cm^{-1}$) coordination modes in **2**. The IR spectrum of **3** indicates characteristic bands of carboxyl groups at 1673 $cm^{-1}$ ($\nu_{as}$) ,1406 $cm^{-1}$ ($\nu_s$) and 1322 $cm^{-1}$ ($\nu_s$). The separations (Δ) between $\nu_{as}$ ($CO_2$) and $\nu_s$ ($CO_2$) illustrate the presence of bidentate (Δ > 250 $cm^{-1}$) coordination mode in **3**. In addition, the absence of strong peaks at ca. 1700 $cm^{-1}$ in **1**, **2** and **3** reveals that all carboxylic groups are deprotonated.[35]

**Magnetic Properties**

The magnetic properties of complexes **2** and **3** are shown in Fig. 3 and Fig. 4, respectively. **2** contains a binuclear Mn2 unit and the $\chi_M$ of **2** increases with decreasing the temperature, reaching a maximum of 0.0095 $cm^3$ $mol^{-1}$ at around 2.0 K, and then decreases quickly. The $\chi_M$T value at 300 K is 13.33 $cm^3$ K $mol^{-1}$, which is larger than the expected value for two high-spin Mn (II) ions[36] ($\chi_M$T = 8.75 $cm^3$ K $mol^{-1}$ $S$ = 5/2, $g$ = 2.0). By decreasing the temperature, the $\chi_M$T gradually decreases by a small amount to *ca.* 26 K, then shows a steep decreasing, reaching 2.76 $cm^3$ K $mol^{-1}$ at 2.0 K, which suggests a dominant antiferromagnetic interaction between Mn(II) centres.[36] Above 100 K, the inverse susceptibility plot *v.s.* temperature is linear, according to the Curie–Weiss law with a Weiss constant, θ = -4.42 K, and a Curie constant, C = 14.28 $cm^3$ K $mol^{-1}$. The negative Weiss constant indicates that there exists predominantly antiferromagnetic interaction between the Mn(II) centres.[37-40]

**3** is a dinuclear Cu2 paddle-wheel complex. As shown in Fig. 4, the $\chi_M$ of **3** increases with decreasing the temperature, and reaches a maximum (0.0033 $cm^3$ $mol^{-1}$) at around 250 K and minimum (0.0006 $cm^3$ $mol^{-1}$) and 54.6 K, respectively. The $\chi_M$T value at 300 K is 0.75 $cm^3$ K $mol^{-1}$, which is consistent to the expected value for the spin-only value of 0.75 $cm^3$ K $mol^{-1}$ ($S$ = 1/2, $g$ = 2.0). With the temperature decreasing, the $\chi_M$T value of **3** reaching a minimum of 0.008 $cm^3$ K $mol^{-1}$ at around 2.0 K. The results illustrate that there exist a dominant antiferromagnetic interaction between Cu(II) centers.[41,42] This magnetic behavior is similar to other Cu2 paddle-wheel complex.[43]

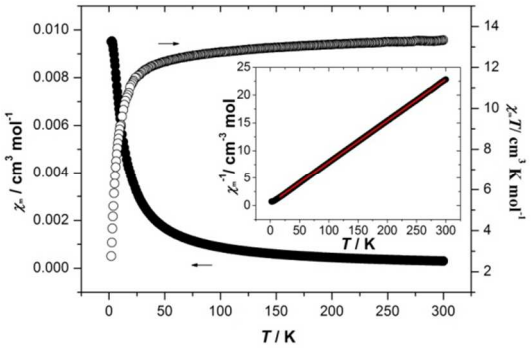


**Fig. 3** Temperature dependence of $\chi_m$T and $\chi_m$ under an applied field of 1000 Oe for **2**. The inset shows the $\chi_m^{-1}$ of **2**.

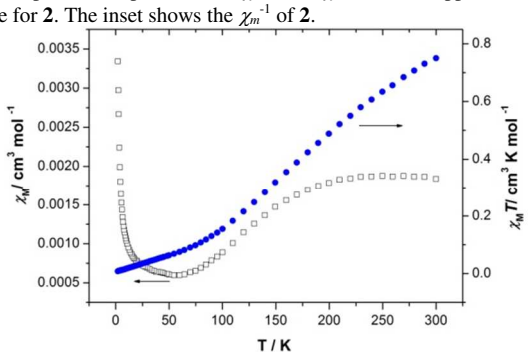


**Fig. 4** Temperature dependence of $\chi_m$T and $\chi_m$ under an applied field of 1000 Oe for **3**.

**DNA binding studies by competitive fluorescence displacement assay**

EB can produce strong fluorescences when intercalated into DNA, and this enhanced fluorescence can be quenched at least partially by the addition of a second molecule.[44] The experimental strategy for determining binding events for EB

based on its fluorescence quenching *via* a competition for binding sites in DNA is a standard method in nucleic acid chemistry. Fluorescence-quenching experiments with EB-bound DNA were performed to determine the binding event of these complexes. No detectable fluorescence emission can be observed for three dinuclear complexes. The fluorescence quench of EB-bound DNA was monitored to investigate the interaction between the complexes and DNA under different concentrations of the three complexes. As shown in Fig. 5, the increasing of the concentration of each complex results in a gradual decrease in fluorescence intensities of the EB-DNA complex, which indicated that all of the three complexes can kick out EB from DNA. This behavior suggests that groove binding interactions will occur between the complexes and DNA.[45,46] For the three complexes, their abilities of kicking out EB from DNA follow the order Cu > Cd >Mn.

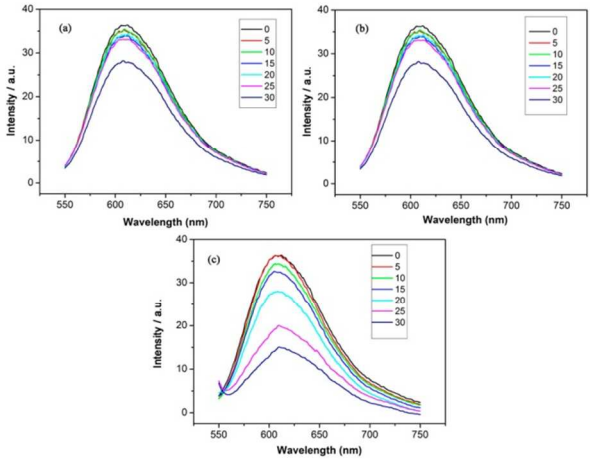


**Fig. 5** Fluorescent emission spectra of EB-DNA complex at various concentration of Mn(II), Cd(II) and Cu(II) complex.

## DNA cleavage

The supercoiled plasmid DNA cleavage by different complexes with three different concentrations was studied in the presence of $H_2O_2$. From Fig. 6, we find that the DNA can be cleaved by the water soluble Cu(II) complex effectively and degrade the supercoiled DNA (Form I) to nicked DNA (Form II) and linear DNA (Form III), but Mn (II) and Cd (II) complexes do not exhibit that ability, regardless of it's concentrations.

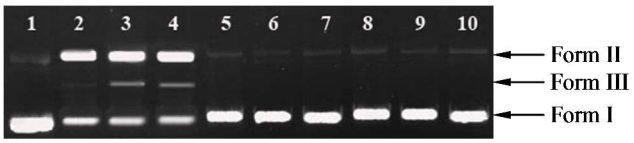


**Fig. 6** Agarose gel electrophoresis of 0.25 μg pBR322 plasmid DNA at 37 °C in 20 mM HEPES at pH 7.0 in the presence of $H_2O_2$ (50 fold of complex) and different complex. Lane 1: DNA control; Lane 2-4: DNA + Cu(II) complex at 0.6, 0.8 and 1.0 μg/μL, respectively; Lane 5-7: DNA + Mn(II) complex at 0.6, 0.8 and 1.0 μg/μL, respectively; Lane 8-10: DNA + Cd(II) complex at 0.6, 0.8 and 1.0 μg/μL, respectively.

As shown in Fig. 7, the cleavage reaction exhibits obviously metal complex concentration dependence. With the increase of complex concentration, supercoiled DNA was gradually transformed into nicked DNA (Form II) and linear DNA (Form III). Incubated with 1 μg/μL Cu for 2 h at pH 7.0, the supercoiled DNA was completely degraded to nicked DNA (72 %) and linear DNA (38 %). Fig. 8 showed that the concentration of $H_2O_2$ had little affect the DNA cleavage, and when the $H_2O_2$ was more than 50 fold of Cu(II) complex, no significant effect of concentration was found for DNA cleavage.

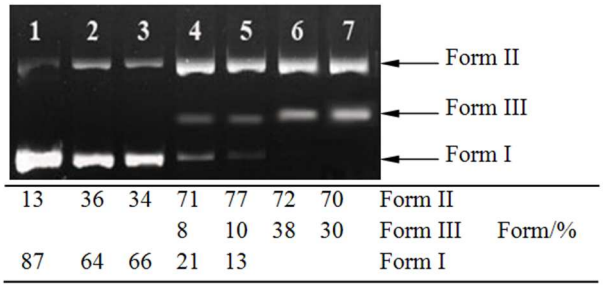


**Fig. 7** Agarose gel showing cleavage of 0.25 μg pBR322 plasmid DNA incubated with Cu(II) complex in 20 mM HEPES, pH 7.0 at 37 °C for 2 h. Lane 1: DNA control; Lane 2-7: DNA + $H_2O_2$ (50 fold of Cu(II) complex) + Cu(II) complex at 0.2, 0.4, 0.6, 0.8, 1.0 and 1.2 μg/μL, respectively.

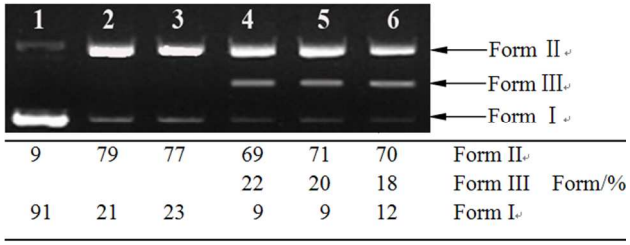


**Fig. 8** Agarose gel electrophoresis of 0.25 μg pBR322 plasmid DNA at 37 °C in 20 mM HEPES at pH 7.0 in the presence of Cu(II) complex (1.0 μg/μL) and $H_2O_2$. Lane 1: DNA control; Lane 2-6: DNA + Cu(II) + $H_2O_2$ at 1, 10, 50, 100 and 150 fold of Cu(II) complex, respectively.

The Cu-mediated DNA cleavage was also dependent on incubating time. As shown in Fig. 9, when incubating time was increased, the intensity of supercioled DNA was decreased. When incubating for 2 h, major supercoiled DNA transformed into nicked DNA (82%) and a small amount transformed into linear DNA (6%). After treated with Cu(II) complex for more than 3 h, supercoiled DNA was finally completely converted into nicked and linear DNA.

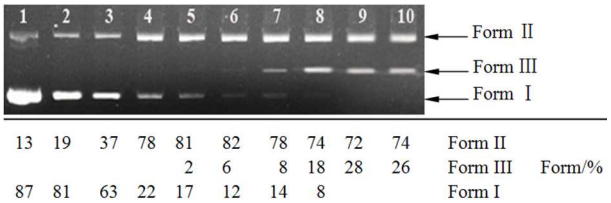


**Fig. 9** Agarose gel electrophoresis of 0.25 μg pBR322 plasmid DNA at 37 °C in 20 mM HEPES at pH 7.0 in the presence of Cu(II) complex (1.0 μg/μL) and $H_2O_2$ (50 fold of Cu(II) complex). Lane 1: DNA control; Lane 2-10: DNA + Cu(II) + $H_2O_2$ for 0, 0.5, 1, 1.5, 2, 2.5, 3, 3.5, 4 h.

In order to further clarify the DNA cleavage mechanism, the Cu-mediated DNA cleavage was investigated in the presence of singlet oxygen scavenger (sodium azide and histidine), hydroxyl radical scavenger (DMSO, tBuOH, ethanol, glycerol), superoxide scavenger (SOD and potassium iodide), chelating agent (EDTA) and binders of DNA minor and major groove (SYBR Green and methyl green). As shown in Fig. 10, sodium azide, histidine, SOD

and potassium iodide did not show any inhibition ability against DNA cleavage and singlet oxygen and superoxide is not likely to be the reactive species. These results were consistent with previous reports.[47] Additionally, no obvious inhibitions was observed in the presence of DMSO, *t*BuOH, ethanol and glycerol, which suggested that hydroxyl radicals were also not responsible for DNA breakage and the possibility of hydroxyl radical in the mechanism could also be ruled out. This result was different from many other DNA cleavage reactions.[48-50] However, EDTA can efficiently inhibit the activity of Cu(II) complex, suggesting that EDTA was able to form a stable complex with Cu(II) ions, which was consistent with $[Cu(L_1)_2(Br)](ClO_4)_5$ reported by Mao et al.[51] In order to investigate whether the higher DNA cleavage ability of Cu(II) complex is relevant to DNA binding ability, the effect of groove binding drugs on the strand scission was also determined. Addition of SYBR green and methyl green, which are known to interact with DNA at minor and major groove, respectively,[52, 53] hardly inhibit DNA cleavage by Cu(II) complex. Based on the results aforementioned, we speculated that, in the absence of any reducing agents, DNA cleavage by Cu(II) complex was likely to proceed via a hydrolytic degradation pathway. The results can partly reflect the relatively strong binding interaction between the Cu(II) complex and DNA, which is consistent with the results of fluorescence spectroscopic studies, showing that the Cu(II) complex has higher DNA binding abilities than the other two complexes.

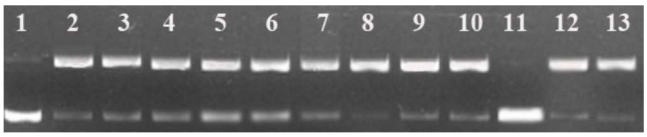


**Fig. 10** Agarose gel electrophoresis of 0.25 μg pBR322 plasmid DNA incubated with Cu(II) complex (1.0 μg/μL) in 20 mM HEPES, pH 7.0 at 37 °C for 2 h. Lane 1: DNA control; Lane 2: DNA + Cu(II), Lane 3-13: DNA + Cu(II) + 150 μM sodium azide, 1.2 mM histidine, 1 M DMSO, 1 M *t*BuOH, 0.7 M ethanol, 0.5 M glycerol, 1000 U $mL^{-1}$ SOD, 0.1 M KI, 0.1 M EDTA, 1000 U SYBR Green and 0.4 mM methyl green.

## Conclusions

Three dinuclear complexes based on two single carboxylic acid ligands have been successfully synthesized. Only the Cu(II) complex shows cleavage activities of double helical DNA. Supercoiled DNA was gradually transformed into nicked DNA (Form II) and linear DNA (Form III) with the increase of concentration of Cu(II) complex. With the increasing of the incubation time, the intensity of supercioled DNA was decreased. The studies of DNA cleavage mechanism showed that singlet oxygen, superoxide and hydroxyl radicals were not likely to be the active species. However, EDTA can inhibit the Cu(II) complex activities efficiently. DNA cleavage by Cu(II) complex was likely to proceed via a hydrolytic degradation pathway.

## Acknowledgment

This work was granted financial support from National Natural Science Foundation of China (Grant 20871063, 21271096), Liaoning BaiQian Wan Talents (2010921066), the Program for Liaoning Excellent Talents in University (LR2011001), the Liaoning Natural Science Foundation, China (201102079), the Innovative Team Project of Department of Education of Liaoning Province, China (LT2011001), and the Liaoning University 211-Projects of the third period.

## Notes and references

[a] *College of Chemistry, Liaoning University, Shenyang 110036 P. R. China E-mail: ceshzb@lnu.edu.cn (Z.-B. Han)*
[b] *College of Light Industry, Liaoning University, Shenyang 110036 P. R. China E-mail: zrg_luck@163.com (R.-G. Zhu)*
† These authors contributed equally to this paper.
†† Electronic Supplementary Information (ESI) available: the $^1$HNMR spectra of the ligands, the TG curves of **1**-**3**, the PXRD patterns of **1**-**3**, and more informations about the crystal structures are available.

1 C. Liu, M. Wang, T. Zhang, H. Sun, *Coord. Chem. Rev.*, 2004, **248**, 147.
2 X. Meng, L. Liu, C. Zhou, L. Wang, C. Liu, *Inorg. Chem.*, 2008, **47**, 6572.
3 J.-R. Li, H.-C. Zhou, *Angew. Chem. Int. Ed.*, 2009, **48**, 8465.
4 M. Demeunynck, C. Bailly, W. D. Wilson, (Eds.), DNA and RNA Binders: from Small Molecules to Drugs, Wiley-VCH: *Weinheim*, Germany, 2003; Vol. 1; p 146.
5 N. Farrell, *Coord. Chem. Rev.*, 2002, **232**, 1.
6 M. Gielen, E. R. T. Tiekink, Metal-lotherapeutic Drugs and Metal-Based Diagnostic Agents: the Use of Metals in Medicine, Wiley: London, U.K., 2005, 359.
7 K. E. Erkkila, D. T. Odom, J. K. Barton, *Chem. Rev.*, 1999, **99**, 2777.
8 D. S. Sigman, A. Mazumder, D. M. Perrin, *Chem. Rev.*, 1993, **93**, 2295.
9 B. Armitage, *Chem. Rev.*, 1998, **98**, 1171.
10 L. J. K. Boerner, J. M. Zaleski, *Curr. Opin. Chem. Biol.*, 2005, **9**, 135.
11 S. O. Kelley, N. M. Jackson, M. G. Hill, J. K. Barton, *Angew. Chem., Int. Ed.*, 1999, **38**, 941.
12 S. O. Kelley, R. E. Holmlin, E. D. A. Stemp, J. K. Barton, *J. Am. Chem. Soc.*, 1997, **119**, 9861.
13 P. K. L. Fu, P. M. Bradley, C. Turro, *Inorg. Chem.*, 2003, **42**, 878.
14 Y. W. Jung, S. J. Lippard, *Chem. Rev.*, 2007, **107**, 1387.
15 J. C. Genereux, A. K. Boal, J. K. Barton, *J. Am. Chem. Soc.*, 2010, **132**, 891.
16 D. S. Sigman, T. W. Bruice, A. Mazumder, C. L. Sutton, *Acc. Chem. Res.*, 1993, **26**, 98.
17 D. S. Sigman, A. Mazumder, D. M. Perrin, *Chem. Rev.*, 1993, **93**, 2295.
18 D. S. Sigman, *Acc. Chem. Res.*, 1986, **19,** 180.
19 D. S. Sigman, D. R. Graham, V. D. Aurora, A. M. Stern, *J. Biol. Chem.*, 1979, 254, 12269.
20 O. Zelenko, J. Gallagher, D.S. Sigman, *Angew. Chem., Int. Ed. Engl.*, 1997, **36**, 2776.
21 G. Pratviel, J. Bernadou, B. Meunier, *Adv. Inorg. Chem.*, 1998, **45**, 251.
22 B. Meunier, *Chem. Rev.*, 1992, **92**, 1411.
23 M. Pitié, C. Boldron, H. Gornitzka, C. Hemmert, B. Donnadieu, B. Meunier, *Eur. J. Inorg. Chem.*, 2003, **3**, 528.
24 W. K. Pogozelski, T. D. Tullius, *Chem. Rev.*, 1998, **98**, 1089.
25 S. A. Ross, M. Pitié, B. Meunier, *Eur. J. Inorg. Chem.*, 1999, **3**, 557.
26 C. Boldron, S. A. Ross, M. Pitié, B. Meunier, *Bioconjug. Chem.*, 2002, **13**, 1013.
27 S. Routier, V. Joanny, A. Zaparucha, H. Vezin, J. P. Catteau, J. L. Bernier, C. J. Bailly, *J. Chem. Soc. Perkin Trans.*, 1998, **2**, 863.
28 S. Dhar, D. Senapati, P. A. N. Reddy, P. K. Das, A. R. Chakravarty, *Chem. Commun.*, 2003, **19**, 2452.
29 D. Shanta, N. Munirathinam, R. C. Akhil, *Dalton Trans.*, 2005, 344.
30 O. Kahn, VCH : New York, 1993.
31 G.M. Sheldrick, SHELXTL, Version 6.10, Bruker Analytical X-ray Systems, Madison, WI, USA, 2001.
32 F. V. Pamatong, C. A. Detmer, J. R. Bocarsly, *J. Am. Chem. Soc.*, 1996, **118**, 5339.

33 Z. B. Han, R. Y. Lu, Y. F. Liang, Y. L. Zhou, Q. Chen, M. H. Zeng, *Inorg. Chem.*, 2012, **51**, 674.

34 A. Gilbert, J. Baggott, CRC Press: Boca Raton, FL. 1991, 87.

35 Z. B. Han, X. N. Cheng, X. M. Chen, *Cryst. Growth & Des.*, 2005, **5**, 695.

36 M. Y. Zhang, W. J. Shan, Z. B. Han, *CrystEngComm*, 2012, **14**, 1568.

37 Y. Li, W. Q. Zou, M. F. Wu, J. D. Lin, F. K. Zheng, Z. F. Liu, S. H. Wang, G. C. Guo and J. S. Huang, *CrystEngComm*, 2011, **13**, 3868.

38 Z. Shen, J. L. Zuo, Z. Yu, Y. Zhang, J. F. Bai, C. M. Che, H. K. Fun, J. J. Vittal and X.-Z. You, *J. Chem. Soc. Dalton Trans.*, 1999, 3393.

39 L. Han, Y. Zhou, X. T. Wang, X. Lia, M. L. Tong, *J. Mol. Struct.*, 2009, **923**, 24.

40 L. F. Ma, L. Y. Wang, Y. Y. Wang, M. Du and J. G. Wang, CrystEngComm, 2009, **11**, 109.

41 Z. B. Han, M. Y. Zhang, D. Q. Yuan, S. Fu, G. X. Zhang and X. F. Wang, CrystEngComm, 2011, **13**, 6945.

42 Z. B. Han, G. X. Zhang, M. H. Zeng, D. Q. Yuan, Q. R. Fang, J. R. Li, J. Ribas and H. C. Zhou, *Inorg. Chem.*, 2010, **49**, 769.

43 B. N. Figgis, R. L. Marlin, *J. Chem. Soc.*, 1956, 3837.

44 C. Liu, J. Zhou, H. Xu, *J. Inorg. Biochem.*, 1998, **71**, 1.

45 B. C. Baguley, *Mol. Cell. Biochem.*, 1982, **43**, 167.

46 A. G. Krishna, D. V. Kumar, B. M. Khan, S. K. Rawal, K. N. Ganesh, *Biochim. Biophys. Acta*, 1998, **1381**, 104.

47 D. D. Li, H. H. Zeng, *Appl. Organometal. Chem.*, 2013, **27**, 89.

48 S. S. Massoud, R. S. Perkins, K. D. Knierim, S. P. Comiskey, K. H. Otero, C. L. Michel, W. M. Juneau, J. H. Albering, F. A. Mautner, W. Xu, *Inorg. Chim. Acta*, 2013, 399, 177.

49 D. M. Kong, J. Wang, L. N. Zhu, Y. W. Jin, X. Z. Li, H. X. Shen, H. F. Mi, *J. Inorg. Biochem.*, 2008, **102**, 824.

50 W. Xu, J. A. Craft, P. R. Fontenot, M. Barens, K. D. Knierim, J. H. Albering, F. A. Mautner, S. S. Massoud, *Inorg. Chim. Acta*, 2011, 273, 159.

51 Y. An, M. L. Tong, L. N. Ji, Z. W. Mao, *Dalton Trans.*, 2006, **17**, 2066.

52 F. B. A. E. Amrani, L. Perelló, J. A. Real, M. González-Alvarez, G. Alzuet, J. Borrás, S. García-Granda, J. Montejo-Bernardo, *J. Inorg. Biochem.*, 2006, **100**, 1208.

53 D. Gibellini, F. Vitone, P. Schiavone, C. Ponti, M. L. Placa, M. C. Re, *J. Clin. Virol.*, 2004, **29**, 282.

## Graph abstract

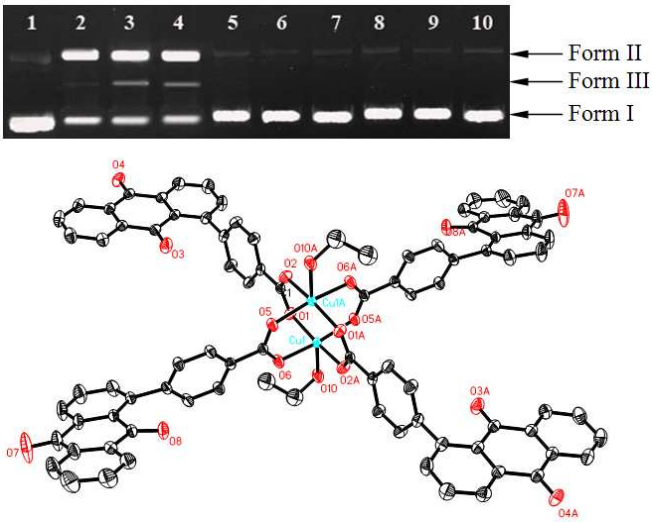


Three dinuclear Cd(II), Mn(II) and Cu(II) complexes have been successfully synthesized under solvothermal conditions. Among them, only the Cu(II) complex has the activities for DNA cleavage.